Am J Transl Res 2015;7(5):932-940
www.ajtr.org /ISSN:1943-8141/AJTR0005279

Original Article

Cordyceps sinensis attenuates renal fibrosis and suppresses BAG3 induction in obstructed rat kidney

Feng Du[1], Si Li[2], Tian Wang[2], Hai-Yan Zhang[3], Zhi-Hong Zong[4], Zhen-Xian Du[2], De-Tian Li[1], Hua-Qin Wang[4], Bo Liu[5], Jia-Ning Miao[5], Xiao-Hui Bian[1]

[1]Department of Nephrology, Shengjing Hospital, China Medical University, Shenyang 110004, China; [2]Department of Endocrinology & Metabolism, The 1st Affiliated Hospital, China Medical University, Shenyang 110001, China; [3]Department of Geriatrics, The 1st Affiliated Hospital, China Medical University, Shenyang 110001, China; [4]Department of Biochemistry & Molecular Biology, China Medical University, Shenyang 110001, China; [5]Key Laboratory of Health Ministry for Congenital Malformation, Shengjing Hospital, China Medical University, Shenyang 110004, China

Received December 23, 2014, Accepted May 2, 2015; Epub May 15, 2015; Published May 30, 2015

Abstract: BAG3 regulates a number of cellular processes, including cell proliferation, apoptosis, adhesion and migration, and epithelial-mesenchymal transition (EMT). However, the role of BAG3 in renal tubular EMT and renal interstitial fibrosis remains elusive. This study aimed to examine the dynamic expression of BAG3 during renal fibrosis, and to investigate the efficacy of *Cordyceps sinensis* (*C. sinensis*) on renal fibrosis. A rat model of unilateral ureteral obstruction (UUO) was established, and the expression of BAG3 and α-SMA, and the efficacy of *C. sinensis* on renal fibrosis induced by UUO were examined. The results showed that UUO led to collagen accumulation, which was significantly suppressed by *C. sinensis*. UUO increased the expression of BAG3 and α-SMA, a mesenchymal marker, while UUO induced BAG3 and α-SMA expression was significantly inhibited by *C. sinensis*. In addition, immunohistochemical staining demonstrated that BAG3 immunoreactivity was restricted to tubular epithelium. In conclusion, BAG3 is a potential target for the prevention and/or treatment of renal fibrosis, and *C. Sinensis* is a promising agent for renal fibrosis.

Keywords: BAG3, *Cordyceps sinensis*, unilateral ureteral obstruction, renal fibrosis

Introduction

Bcl-2-associated athanogene 3 (BAG3) is a member of the BAG domain containing co-chaperone family, which is initially identified as an interaction partner of Bcl-2 and characterized by the interaction with multiple partners such as heat shock proteins (HSPs), Bcl-2, Raf, and steroid hormone receptors [1, 2]. In human, BAG3 is constitutively expressed in the skeletal muscle and the heart [2-4]. BAG3 expression is induced in different types of cells in response to various cellular stress, such as the exposure to high temperature, HIV infection, oxidants, heavy metal exposure, and some chemotherapeutic drugs [5-10]. BAG3 expression is also upregulated in several tumors, such as leukemia, lymphoma, myeloma, pancreas and thyroid carcinomas [10-14]. BAG3 plays a regulatory role in a number of cellular processes, including cell proliferation, apoptosis, adhesion and migration, epithelial-mesenchymal transition (EMT), autophagy activation, and virus infection [15]. BAG3 has also been reported to be implicated in autophagy [16-21]. Furthermore, very recently we demonstrated that BAG3 regulated EMT of thyroid cancer cells [22]. However, the role of BAG3 in renal tubulointerstitial fibrosis has not been explored.

Renal tubulointerstitial fibrosis is a pivotal event in the progression of chronic kidney disease, which is characterized by increased accumulation of extracellular matrix (ECM) accumulation. EMT of tubular epithelial cells into myofibroblasts is one of the important pathogenic mechanisms of renal interstitial fibrosis [23-25]. During the EMT process, epithelial cells lose epithelial surface markers and cell polarity, coincided with the expression of mesenchymal

markers and the acquirement of mesenchymal phenotype [25]. Experimentally, unilateral ureteral obstruction (UUO) has been identified as one of the most characterized renal fibrosis model, in which EMT plays an important role [26].

Cordyceps is one of the most valuable traditional Chinese medicine which is composed of the dried fungus *Cordyceps sinensis* (*C. sinensis*) growing on the larva of caterpillar [27]. *C. sinensis* is extensively used by Chinese physicians to treat chronic renal diseases, and it stimulates immune system and possesses antioxidative activities [28, 29]. In the present study, we evaluated progressive renal interstitial fibrosis in UUO model to examine the dynamic changes of BAG3 in obstructive nephropathy as the first step to investigate the role of BAG3 during the pathogenesis of renal interstitial fibrosis. In addition, we investigated the efficacy of *C. sinensis* on renal interstitial fibrosis in the rat model of UUO.

Materials and methods

Unilateral ureteral obstruction (UUO) model

All animal experiments were approved by Shengjing hospital, China Medical University. The unilateral ureteral obstruction (UUO) model was established in 8-week-old male Sprague-Dawley rats (weight 250-300 g). Animals were anesthetized with an intraperitoneal injection of ketamine (75 mg/kg body weight). After the abdomen was opened with a midline incision, UUO was performed by ligating the left ureter with 4.0 silk at both proximal and distal points. Ureter was severed between these two ligation points. In sham group, ureter was isolated but not ligated. The abdominal cavity was then closed in layers. Rats were killed at days 7, 14 and 21 after the operation (10 in each group at each time point).

C. sinensis treatment

Artificially cultured *C. sinensis* (trade name Corbrin capsule, also called "Bailing Jiaonang" in Chinese Pharmacopoeia) was provided by Hangzhou Huadong Pharmaceutical Company (Hangzhou, China), and was dissolved in 1 ml of normal saline. Rats were given at a dose of 1.5 g/kg day by intragastric administration from the day of the operation and the control rats were given same amount of normal saline.

Tissue preparation

Under anesthesia, the kidneys were taken out from the rats. A small portion of the renal tissue was taken and fixed in 4% paraformaldehyde for histology and immunohistochemical assays. The remained renal tissues were flash-frozen by liquid nitrogen, and stored at -80 C for real-time PCR and Western blot assay.

Fibrotic scoring

Paraffin sections (5 μm) of the kidneys were stained with Masson's trichrome. The interstitial collagen deposition was analyzed by using a standard point-counting method as previously described [7] and expressed as the percentage of the fibrotic grid points to the total grid points examined. These examinations evaluated the areas overlying the tubular basement membrane and interstitial space while avoiding glomeruli and large vessels. In each section with Masson's trichrome staining, 10 fields were digitized and scanned at 400x magnification by using NIS-Elements BR 2.10 image analysis software (Nikon, Tokyo, Japan). Using a grid superimposed on the image, the number of blue collagen staining points was counted, and the percentage of blue collagen area in the examined tubulointerstitial was measured. Average of this ratio represented relative area of renal interstitium on each slide.

Measurement of hydroxyproline concentration

Hydroxyproline concentration was determined in kidney lysates as described previously [30]. Briefly, tissue was lysed in 1% Triton, 4 mM EDTA, 1% protease inhibitor cocktail (Roche) and homogenized with a prechilled mortar and pestle. After centrifugation at 10,000 rpm at 4C, both the supernatant and pellet fractions were hydrolyzed in 6 M HCl (110C, 6 h). The data were expressed as μg of collagen per mg total lysate protein using the Bio-Rad Protein Assay (Bio-Rad).

Immunohistochemistry

Immunohistochemical staining was performed by a peroxidase labeled streptavidin-biotin-complex technique. The kidney sections were preincubated with 5% BSA-PBS for 5 min. Endogenous biotin was blocked with avidin and biotin for 10 min, respectively. Sections were subsequently incubated with the mouse mono-

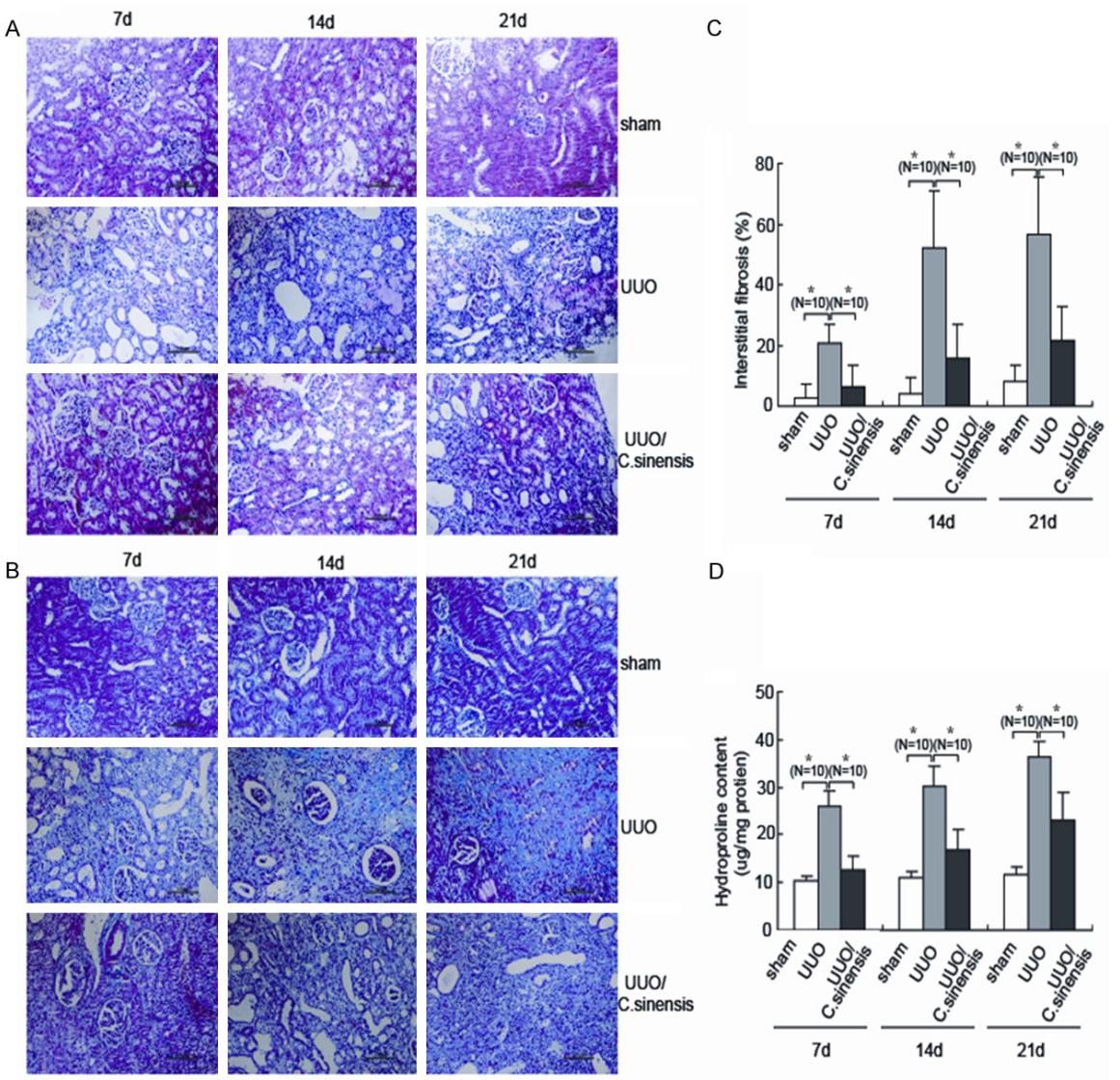

Figure 1. *C. sinensis* had nephroprotective effects in UUO rats. A. Representative images of HE staining of the kidney of rats on days 7, 14, and 21 after the sham, UUO operation, or UUO operation treated with *C. sinensis*. Scale bar: 100 μm. B. Representative images of Masson staining of the kidney of rats on days 7, 14, and 21 after the sham, UUO operation, or UUO operation treated with *C. sinensis*. Scale bar: 100 μm. C. The percentage of renal interstitial fibrosis in the kidneys (n = 10). D. The quantitative data of hydroxyproline content in the kidneys (n = 10). *, $p < 0.05$.

clonal antibody against BAG3 (Enzo Life Sciences) for 1 h. After washing with PBS, the sections were incubated with biotinylated goat anti-mouse IgG in PBS containing 2% normal goat serum for 30 min, followed by incubation with peroxidase labeled streptavidin-biotin-complex for 30 min, and final incubation with diaminobenzidine tetrahydrochloride in the presence of 3% hydrogen peroxide for 10 min. All reactions were performed at room temperature. Sections were finally counterstained with Harris hematoxylin, dehydrated and mounted with Pertex.

Western blot analysis

The tissues were lysed in Laemmli buffer, and the proteins of the lysates were separated by SDS-polyacrylamide gel electrophoresis, transferred to PVDF membranes and probed using rabbit antibody against BAG3 (Abcam), mouse antibody against α-SMA (Sigma-Aldrich) and mouse antibody against GAPDH (Sigma-Aldrich). The blots were incubated with secondary antibodies. Positive immunoreactive bands were detected by enhanced chemiluminescence (ECL), and analyzed by densitometry.

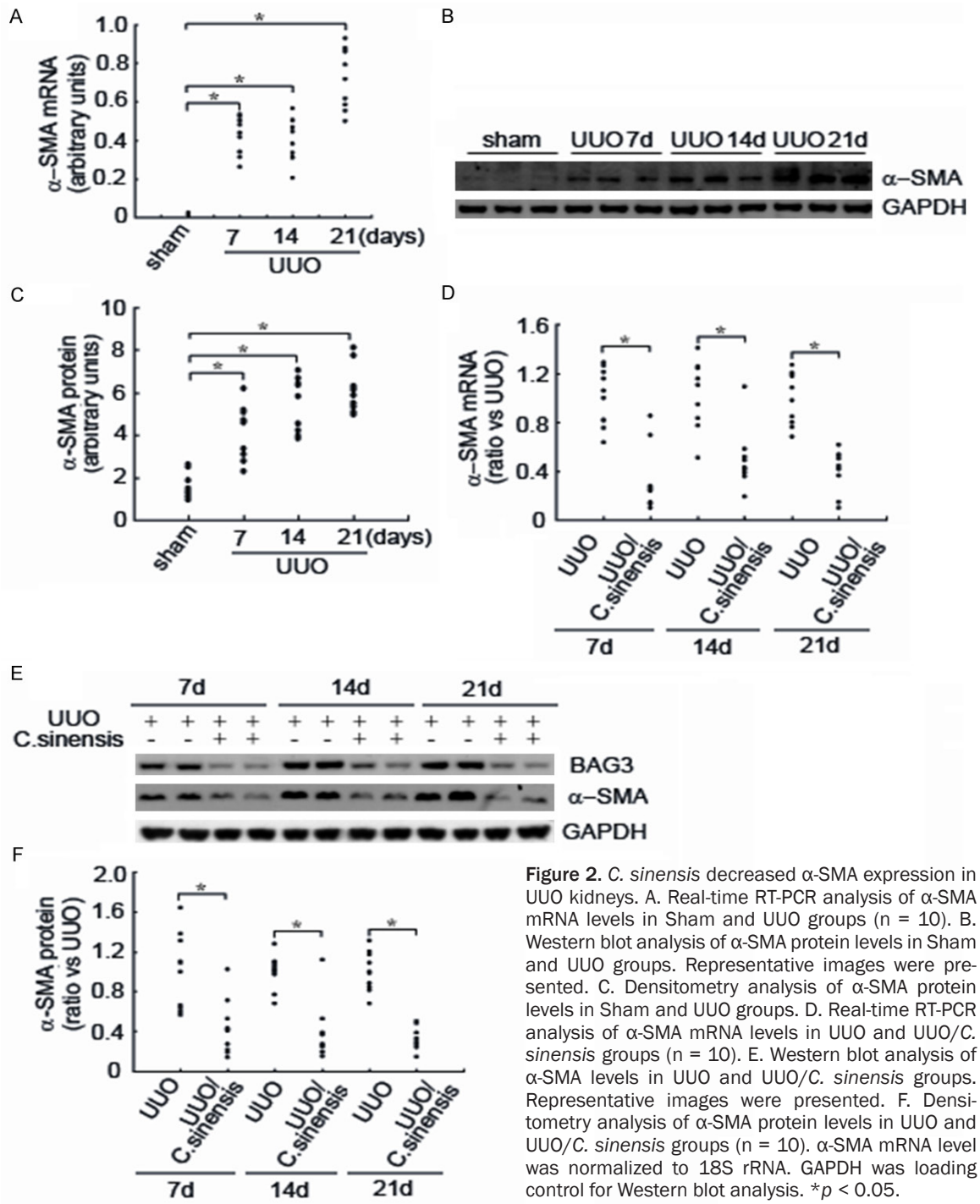

Figure 2. *C. sinensis* decreased α-SMA expression in UUO kidneys. A. Real-time RT-PCR analysis of α-SMA mRNA levels in Sham and UUO groups (n = 10). B. Western blot analysis of α-SMA protein levels in Sham and UUO groups. Representative images were presented. C. Densitometry analysis of α-SMA protein levels in Sham and UUO groups. D. Real-time RT-PCR analysis of α-SMA mRNA levels in UUO and UUO/*C. sinensis* groups (n = 10). E. Western blot analysis of α-SMA levels in UUO and UUO/*C. sinensis* groups. Representative images were presented. F. Densitometry analysis of α-SMA protein levels in UUO and UUO/*C. sinensis* groups (n = 10). α-SMA mRNA level was normalized to 18S rRNA. GAPDH was loading control for Western blot analysis. *$p < 0.05$.

Real-time polymerase chain reaction

Total RNA was extracted from tissues using Trizol (Invitrogen, Carlsbad) and reverse transcription. quantitative real-time PCR with 18s ribosomal RNA (18s rRNA) as an internal control was performed using SYBR green PCR master mix kit (Applied Biosystems, Foster City) on an ABI 7500 real-time PCR thermal cycler (Applied Biosystems). The messenger RNA (mRNA) expressions of test genes were normalized to 18s rRNA levels. The primers were as follows: BAG3, forward primer 5'-CATCCAGGAGTGCTGAAAGTG-3', reverse primer 5'-TCTGAACCTTCCTGACACCG-3'; α-SMA: forward primer 5'-CTTGCTAACGGAGGCG-3', reverse primer 5'-TCCAGAGTCCAGCACAATA-3'.

Statistical analysis

Data were expressed as mean values ± standard deviation (SD) with N as the number of experiments. The statistical significance of differences among groups was compared by analysis of variance (ANOVA), and correlation analysis between two variables was done by Pearson correlation analysis. $P < 0.05$ was considered significant difference.

Results

C. sinensis attenuated tubular fibrosis in UUO rats

HE staining demonstrated that renal tubules were compact and well organized in the kidneys from the sham rats. By contrast, renal tubular structure was gradually damaged, and renal interstitial edema and dilation of renal tubules were detected at different time points in UUO rats (**Figure 1A**). Masson's trichrome staining demonstrated that there was no interstitial collagen deposition (blue stain) in the kidneys from the sham rats. The appearance of Masson stain in the kidney section starts at 7d after UUO operation, which was progressively increased with prolonged obstruction (**Figure 1B**). Renal interstitial fibrosis area in the UUO group was significantly larger than that of the sham group (**Figure 1C**). In addition, hydroxylproline content was significantly increased on 7d after UUO, and demonstrated time-dependent increase on 14d and 21d after UUO (**Figure 1D**). Administration of *C. sinensis* significantly attenuated renal tubular damage (**Figure 1A**), tubular fibrosis (**Figure 1B-D**) and accumulation of collagen I (**Figure 1D**) induced by UUO.

C. sinensis suppressed renal α-SMA expression in UUO rats

The marker of tubulointerstitial fibrosis α-SMA was measured by real-time RT-PCR and Western blot analysis. α-SMA mRNA expression level was significantly increased in the obstructed kidneys compared with the sham operated kidneys on 7 days after UUO induction (**Figure 2A**). Western blot analysis demonstrated that α-SMA protein expression level was significantly increased in UUO group after the surgery (**Figure 2B**, **2C**). C. sinensis significantly suppressed UUO induced α-SMA mRNA expression (**Figure 2D**). Western blot analysis confirmed that α-SMA protein expression in UUO rats was suppressed by the administration of *C. sinensis* (**Figure 2E**, **2F**).

C. sinensis suppressed BAG3 expression in UUO rats

By RT-PCR analysis, a significant increase in BAG3 mRNA level in UUO group was detected on 7d after the surgery, compared to the sham group, and BAG3 mRNA expression continued to increase with prolonged obstruction (**Figure 3A**). Consistently, Western blot analysis demonstrated that BAG3 protein expression level was significantly augmented in UUO-operated kidneys (**Figure 3B**, **3C**). *C. sinensis* significantly inhibited UUO-mediated upregulation of BAG3 mRNA expression (**Figure 3D**). Western blot analysis confirmed that BAG3 protein expression in UUO rats was suppressed by the administration of *C. sinensis* (**Figure 3E**, **3F**).

BAG3 expression was specifically increased in tubular epithelium in UUO rats

Immunohistochemical analysis showed that no or little BAG3 staining was observed in the kidney sections from sham-operated control rats, while positive BAG3 staining appeared in renal tubular epithelial cells at 7d after UUO operation and became stronger at 14d and 21d after the operation (**Figure 4A**). It should be noted that positive BAG3 immunostaining was limited in tubular epithelium, and BAG3 immunostaining was weak after the administration of *C. sinensis* (**Figure 4A**).

α-SMA immunostaining was also performed for kidney sections. Almost no α-SMA immunostaining was detected in the kidney sections from the sham rats, while strong α-SMA immunostaining appeared in tubular epithelium of the kidney sections from UUO rats at 7d, and further increased afterward (**Figure 4B**). Administration of C. sinensis significantly inhibited the induction of α-SMA mediated by UUO operation (**Figure 4B**).

Discussion

With the progression of renal fibrosis, in the obstructed kidney tubular epithelial cells are differentiated into myofibroblasts as a process of EMT, leading to increased α-SMA expression and the accumulation of ECM proteins [31]. In this study we established UUO model for induc-

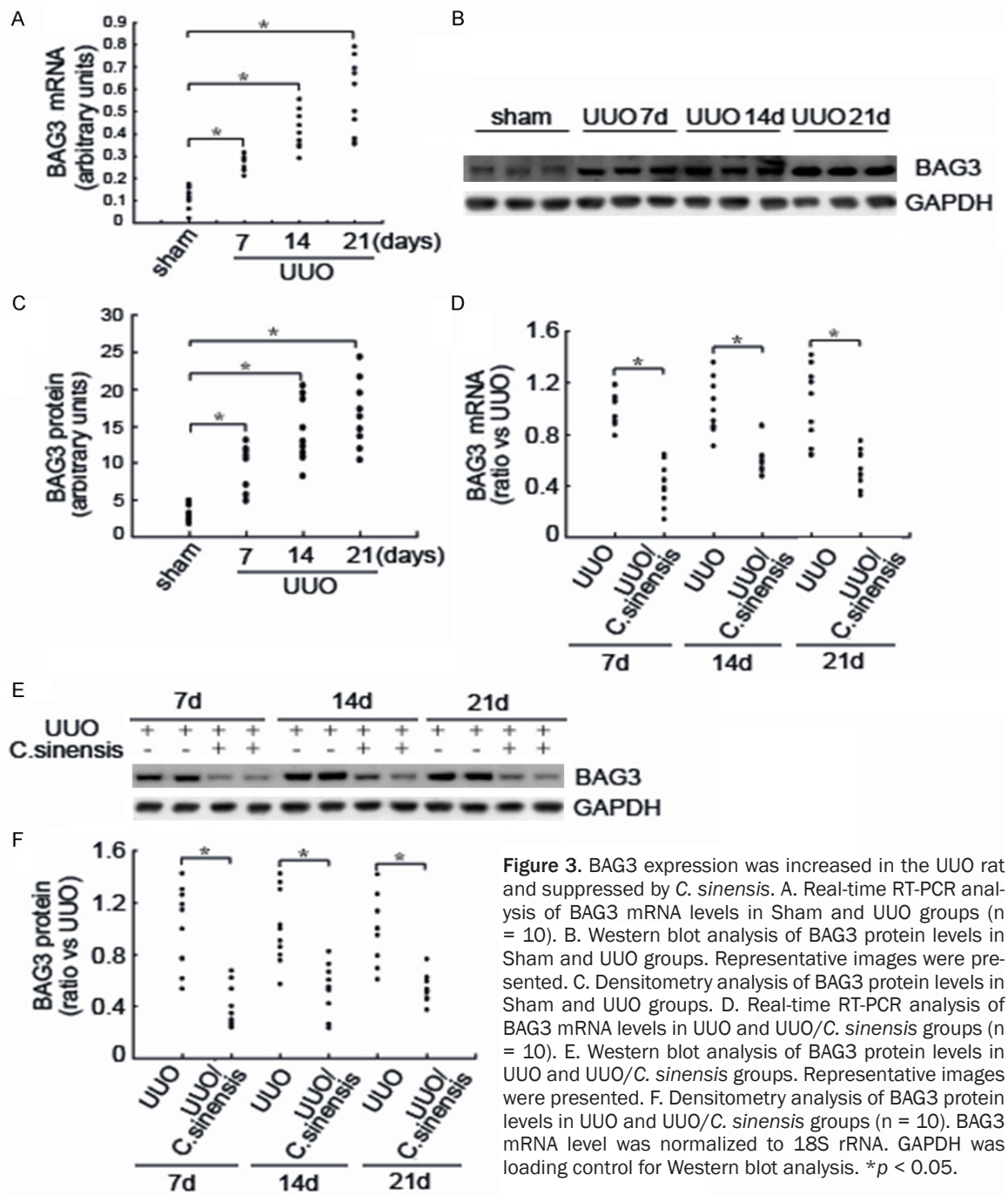

Figure 3. BAG3 expression was increased in the UUO rat and suppressed by *C. sinensis*. A. Real-time RT-PCR analysis of BAG3 mRNA levels in Sham and UUO groups (n = 10). B. Western blot analysis of BAG3 protein levels in Sham and UUO groups. Representative images were presented. C. Densitometry analysis of BAG3 protein levels in Sham and UUO groups. D. Real-time RT-PCR analysis of BAG3 mRNA levels in UUO and UUO/*C. sinensis* groups (n = 10). E. Western blot analysis of BAG3 protein levels in UUO and UUO/*C. sinensis* groups. Representative images were presented. F. Densitometry analysis of BAG3 protein levels in UUO and UUO/*C. sinensis* groups (n = 10). BAG3 mRNA level was normalized to 18S rRNA. GAPDH was loading control for Western blot analysis. $*p < 0.05$.

ing renal fibrosis, HE and Masson staining revealed obvious renal interstitial fibrosis in UUO group, and RT-PCR and Western blot analysis demonstrated the induction of α-SMA in the obstructed kidneys, confirming that tubulointerstitial fibrosis had been successfully induced in our UUO model.

As a valuable traditional herbal medicine, *C. sinensis* has been commonly used to replenish the kidney function and treat renal dysfunction and renal failure. Co-treatment with *C. sinensis* is superior to traditional immunosuppressive drugs alone to benefit chronic allograft nephropathy patients, and *C. sinensis* is currently used for clinical therapy for chronic allograft nephropathy or long-term therapy for renal transplant patients in China [32, 33]. In the present study, *C. sinensis* treatment significantly improved renal fibrosis as assessed by Masson staining,

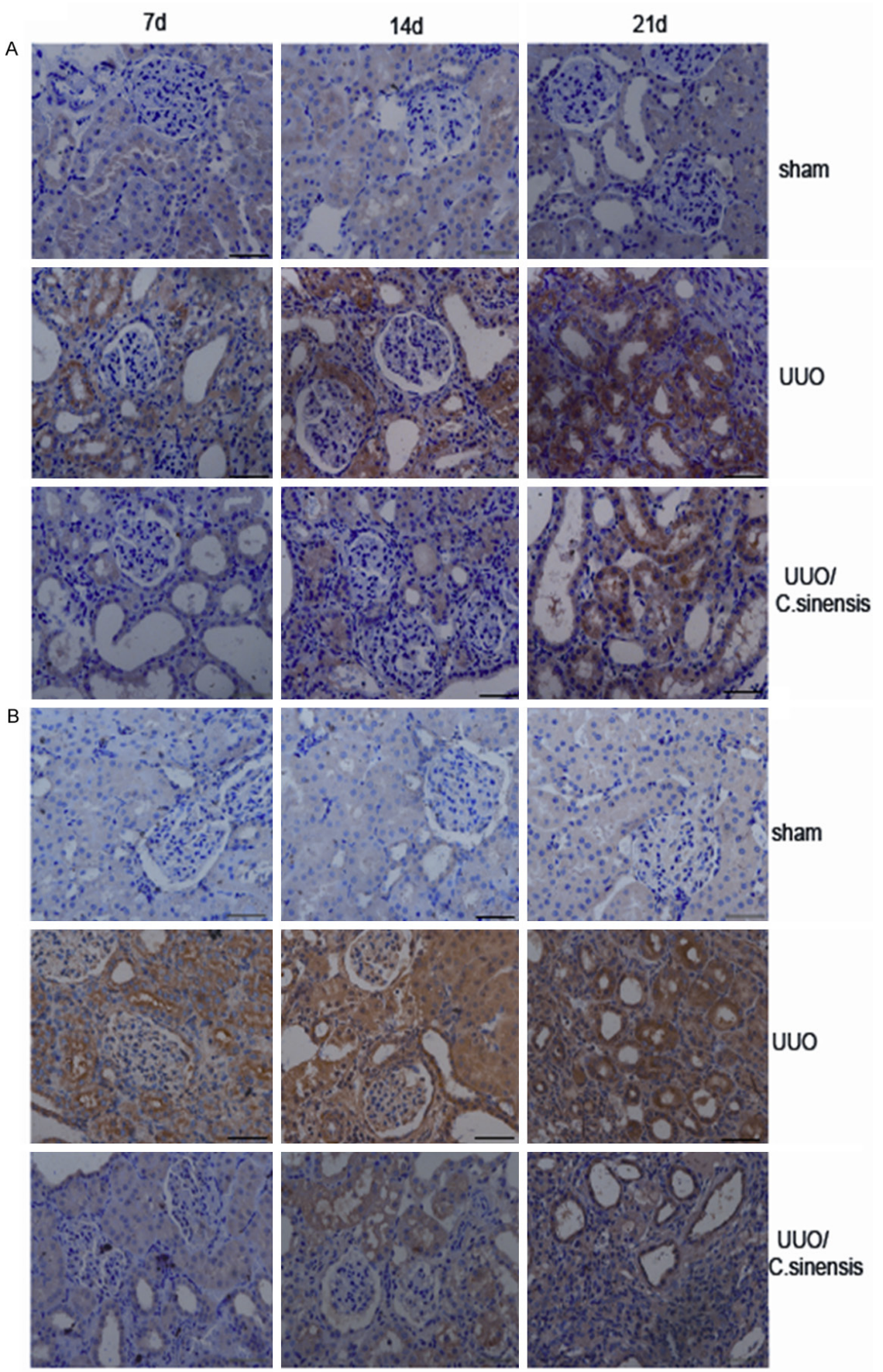
7d
14d
21d
A
sham
UUO
UUO/
C.sinensis
B
sham
UUO
UUO/
C.sinensis

Figure 4. Immunohistochemical staining of BAG3 and α-SMA in rat kidneys. A. Representative images of BAG staining in the kidney of rats on days 7, 14, and 21 after the sham, UUO operation, or UUO operation treated with *C. sinensis*. B. Representative images of α-SMA staining in the kidney of rats on days 7, 14, and 21 after the sham, UUO operation, or UUO operation treated with *C. sinensis*. Scale bar: 20 μm.

α-SMA immunostaining, and procted the kidney structure following UUO operation.

BAG3 is involved in a number of cellular processes, including cell proliferation, cell cycle progression, apoptosis, angiogenesis, selective autophagy, adhesion and migration [34]. It seems that the induction of BAG3 is a protective mechanism in response to stressful stimuli, as decreased induction of BAG3 promoted cell death in various human cell models [5, 9, 10]. However, the relationship between the expression of BAG3 and fibrotic conditions is unclear. This study, for the first time, investigated the dynamic alterations of BAG3 expression in response to injurious stimuli and demonstrated that BAG3 was upregulated in UUO-induced tubulointerstitial fibrosis. In addition, immunohistochemical staining showed that the upregulation of BAG3 was restricted to tubular epithelium. In addition, we found that *C. sinensis* improved renal fibrosis in UUO model, accompanied by decreased BAG3 expression. These data strongly indicate the pathogenic role of BAG3 in tubulointerstitial fibrosis.

In summary, our study suggested that BAG3 should be considered as a potential target for the prevention and/or treatment of tubulointerstitial fibrosis, and *C. sinensis* may be a promising agent to combat renal fibrosis.

Acknowledgements

This study was supported by National Natural Science Foundation of China (No. 31170727, 31170745 and 81301838).

Disclosure of conflict of interest

None.

Address correspondence to: Dr. Feng Du, Department of Nephrology, Shengjing Hospital, China Medical University, Shenyang 110004, China. Tel: +86-24-96615-25111; Fax: +86-24-96615-25814; E-mail: dolphine_doctor@163.com

References

[1] Antoku K, Maser RS, Scully WJ Jr, Delach SM, Johnson DE. Isolation of bcl-2 binding proteins that exhibit homology with bag-1 and suppressor of death domains protein. Biochem Biophys Res Commun 2001; 286: 1003-1010.

[2] Doong H, Price J, Kim YS, Gasbarre C, Probst J, Liotta LA, Blanchette J, Rizzo K, Kohn E. Cair-1/bag-3 forms an egf-regulated ternary complex with phospholipase c-gamma and hsp70/hsc70. Oncogene 2000; 19: 4385-4395.

[3] Homma S, Iwasaki M, Shelton GD, Engvall E, Reed JC, Takayama S. Bag3 deficiency results in fulminant myopathy and early lethality. Am J Pathol 2006; 169: 761-773.

[4] Hishiya A, Kitazawa T, Takayama S. Bag3 and hsc70 interact with actin capping protein capz to maintain myofibrillar integrity under mechanical stress. Circ Res 2010; 107: 1220-1231.

[5] Pagliuca MG, Lerose R, Cigliano S, Leone A. Regulation by heavy metals and temperature of the human bag-3 gene, a modulator of hsp70 activity. FEBS Lett 2003; 541: 11-15.

[6] Bonelli P, Petrella A, Rosati A, Romano MF, Lerose R, Pagliuca MG, Amelio T, Festa M, Martire G, Venuta S, Turco MC, Leone A. Bag3 protein regulates stress-induced apoptosis in normal and neoplastic leukocytes. Leukemia 2004; 18: 358-360.

[7] Lin SL, Chen RH, Chen YM, Chiang WC, Lai CF, Wu KD, Tsai TJ. Pentoxifylline attenuates tubulointerstitial fibrosis by blocking smad3/4-activated transcription and profibrogenic effects of connective tissue growth factor. J Am Soc Nephrol 2005; 16: 2702-2713.

[8] Tabuchi Y, Ando H, Takasaki I, Feril LB Jr, Zhao QL, Ogawa R, Kudo N, Tachibana K, Kondo T. Identification of genes responsive to low intensity pulsed ultrasound in a human leukemia cell line molt-4. Cancer Lett 2007; 246: 149-156.

[9] Wang HQ, Liu HM, Zhang HY, Guan Y, Du ZX. Transcriptional upregulation of bag3 upon proteasome inhibition. Biochem Biophys Res Commun 2008; 365: 381-385.

[10] Du ZX, Zhang HY, Meng X, Gao YY, Zou RL, Liu BQ, Guan Y, Wang HQ. Proteasome inhibitor mg132 induces bag3 expression through activation of heat shock factor 1. J Cell Physiol 2009; 218: 631-637.

[11] Romano MF, Festa M, Pagliuca G, Lerose R, Bisogni R, Chiurazzi F, Storti G, Volpe S, Venuta S, Turco MC, Leone A. Bag3 protein controls b-chronic lymphocytic leukaemia cell apoptosis. Cell Death Differ 2003; 10: 383-385.

[12] Romano MF, Festa M, Petrella A, Rosati A, Pascale M, Bisogni R, Poggi V, Kohn EC, Venuta S,

Turco MC, Leone A. Bag3 protein regulates cell survival in childhood acute lymphoblastic leukemia cells. Cancer Biol Ther 2003; 2: 508-510.

[13] Chiappetta G, Ammirante M, Basile A, Rosati A, Festa M, Monaco M, Vuttariello E, Pasquinelli R, Arra C, Zerilli M, Todaro M, Stassi G, Pezzullo L, Gentilella A, Tosco A, Pascale M, Marzullo L, Belisario MA, Turco MC, Leone A. The anti-apoptotic protein bag3 is expressed in thyroid carcinomas and modulates apoptosis mediated by tumor necrosis factor-related apoptosis-inducing ligand. J Clin Endocrinol Metab 2007; 92: 1159-1163.

[14] Wang HQ, Liu BQ, Gao YY, Meng X, Guan Y, Zhang HY, Du ZX. Inhibition of the jnk signalling pathway enhances proteasome inhibitor-induced apoptosis of kidney cancer cells by suppression of bag3 expression. Br J Pharmacol 2009; 158: 1405-1412.

[15] Gamerdinger M, Hajieva P, Kaya AM, Wolfrum U, Hartl FU, Behl C. Protein quality control during aging involves recruitment of the macroautophagy pathway by bag3. EMBO J 2009; 28: 889-901.

[16] Carra S, Brunsting JF, Lambert H, Landry J, Kampinga HH. Hspb8 participates in protein quality control by a non-chaperone-like mechanism that requires eif2{alpha} phosphorylation. J Biol Chem 2009; 284: 5523-5532.

[17] Carra S. The stress-inducible hspb8-bag3 complex induces the eif2alpha kinase pathway: Implications for protein quality control and viral factory degradation? Autophagy 2009; 5: 428-429.

[18] Carra S, Seguin SJ, Landry J. Hspb8 and bag3: A new chaperone complex targeting misfolded proteins to macroautophagy. Autophagy 2008; 4: 237-239.

[19] Carra S, Seguin SJ, Lambert H, Landry J. Hspb8 chaperone activity toward poly(q)-containing proteins depends on its association with bag3, a stimulator of macroautophagy. J Biol Chem 2008; 283: 1437-1444.

[20] Fuchs M, Poirier DJ, Seguin SJ, Lambert H, Carra S, Charette SJ, Landry J. Identification of the key structural motifs involved in hspb8/hspb6-bag3 interaction. Biochem J 2009; 425: 245-255.

[21] Liu BQ, Du ZX, Zong ZH, Li C, Li N, Zhang Q, Kong DH, Wang HQ. Bag3-dependent noncanonical autophagy induced by proteasome inhibition in hepg2 cells. Autophagy 2013; 9: 905-916.

[22] Li N, Du ZX, Zong ZH, Liu BQ, Li C, Zhang Q, Wang HQ. Pkcdelta-mediated phosphorylation of bag3 at ser187 site induces epithelial-mesenchymal transition and enhances invasiveness in thyroid cancer cells. Oncogene 2013; 32: 4539-4548.

[23] Lee SY, Kim SI, Choi ME. Therapeutic targets for treating fibrotic kidney diseases. Transl Res 2015; 165: 512-530.

[24] Liu Y. Cellular and molecular mechanisms of renal fibrosis. Nat Rev Nephrol 2011; 7: 684-696.

[25] Liu Y. New insights into epithelial-mesenchymal transition in kidney fibrosis. J Am Soc Nephrol 2010; 21: 212-222.

[26] Picard N, Baum O, Vogetseder A, Kaissling B, Le Hir M. Origin of renal myofibroblasts in the model of unilateral ureter obstruction in the rat. Histochem Cell Biol 2008; 130: 141-155.

[27] Li SP, Zhao KJ, Ji ZN, Song ZH, Dong TT, Lo CK, Cheung JK, Zhu SQ, Tsim KW. A polysaccharide isolated from cordyceps sinensis, a traditional chinese medicine, protects pc12 cells against hydrogen peroxide-induced injury. Life Sci 2003; 73: 2503-2513.

[28] Jordan JL, Sullivan AM, Lee TD. Immune activation by a sterile aqueous extract of cordyceps sinensis: Mechanism of action. Immunopharmacol Immunotoxicol 2008; 30: 53-70.

[29] Li SP, Li P, Dong TT, Tsim KW. Anti-oxidation activity of different types of natural cordyceps sinensis and cultured cordyceps mycelia. Phytomedicine 2001; 8: 207-212.

[30] Chung SD, Lai TY, Chien CT, Yu HJ. Activating nrf-2 signaling depresses unilateral ureteral obstruction-evoked mitochondrial stress-related autophagy, apoptosis and pyroptosis in kidney. PLoS One 2012; 7: e47299.

[31] Chevalier RL, Forbes MS, Thornhill BA. Ureteral obstruction as a model of renal interstitial fibrosis and obstructive nephropathy. Kidney Int 2009; 75: 1145-1152.

[32] Zhang Z, Wang X, Zhang Y, Ye G. Effect of cordyceps sinensis on renal function of patients with chronic allograft nephropathy. Urol Int 2011; 86: 298-301.

[33] Ding C, Tian PX, Xue W, Ding X, Yan H, Pan X, Feng X, Xiang H, Hou J, Tian X. Efficacy of cordyceps sinensis in long term treatment of renal transplant patients. Front Biosci (Elite Ed) 2011; 3: 301-307.

[34] Zhu H, Liu P, Li J. Bag3: A new therapeutic target of human cancers? Histol Histopathol 2012; 27: 257-261.